STRESS CONCENTRATIONS CAUSED BY GRAIN BOUNDARY SLIDING IN METALS UNDERGOING POWER-LAW CREEP

C. W. Lau and A. S. Argon*

INTRODUCTION

At elevated temperatures where crystalline metals can undergo diffusion controlled steady state creep according to a non-linear viscosity law, and where grain boundary sliding is encountered, fracture frequently becomes intergranular. Such fracture frequently starts by either crack nucleation at triple-point grain junctions or by pore formation at non-deformable inclusions situated at grain boundaries [1,2]. It has long been recognized that this is a result of stress concentrations that arise at triple points and at hard inclusions where the free sliding of the boundaries are obstructed. In this paper we discuss how such stress concentrations can be calculated in non-linearly creeping matter.

METHOD OF ANALYSIS

Creep deformation in a polycrystalline metal combines grain boundary sliding with both power-law creep within the grains and diffusional flow of matter between grain boundaries. We will be interested here in only the high stress range where grain boundary sliding and power law creep dominate. In this range the basic creep equation is of the type

$$\dot{\varepsilon} = A\sigma^n \tag{1}$$

where $\dot{\varepsilon}$ is the steady state tensile creep rate, σ is the tensile stress, $n(>3)$ is an empirical material constant, and A incorporates a Boltzmann factor [3]. In a more general stress state the above expression is taken as a relation between the equivalent strain rate $\dot{\varepsilon}_e$ and the equivalent stress σ_e.

Stresses at a Triple Grain Junction

The polycrystalline metal is visualized as a network of regular hexagonal grains. Since at steady state creep grain boundaries are assumed to slide freely, the shear stress along any boundary is zero. Within any grain the deformation obeys a constitutive equation for power-law creep given by

$$\dot{\varepsilon}_{ij} = \frac{3}{2}\ \alpha\ (\sigma_e)^{n-1}\ s_{ij} \tag{2}$$

*Department of Mechanical Engineering, M.I.T., Cambridge, Mass., 02139, U.S.A.

where $\dot{\varepsilon}_{ij}$ is the local strain rate tensor for steady state creep, α incorporates a Boltzmann factor, n is the exponent defined in (1) above, σ_e is the Mises equivalent stress, and s_{ij} is the stress deviator, both defined as

$$s_{ij} \equiv \sigma_{ij} - \frac{1}{3}\sigma_{kk}\delta_{ij} \tag{3}$$

$$\sigma_e \equiv \sqrt{\frac{3}{2} s_{ij} s_{ij}} \tag{4}$$

Of interest is the stress and strain rate singularity at the triple point shown in Figure 1 which also gives the boundary conditions appropriate for far field tensile loading. We start by first noting the correspondence between velocities and displacements, and between strain rates and strains, in solutions of boundary value problems with prescribed tractions for non-linearly viscous materials and non-linearly hardening materials obeying constitutive equations of similar form. Our problem can then be solved by extending the method first developed by Hutchinson [4] to obtain the singular field of stress and strain around crack tips in homogeneous, isotropic continua obeying a power-law hardening behaviour.

Choosing a coordinate system centred at the triple point as shown in Figure 1, a stress function $\Phi(r,\theta)$ is introduced from which stresses are obtainable in the usual manner. The governing equation for deformation for grains I and II can then be written by combining the equilibrium equation, the compatibility equation for small strain, and the non-linear constitutive equation given by (2) (with $\dot{\varepsilon}_{ij}$ replaced by ε_{ij}). The dominant solution at the triple point is of the form

$$\phi(r,\theta) = Kr^s\tilde{\phi}(\theta) \tag{5}$$

where K is a scale factor, s is an unknown exponent describing the dominant singularity in stress and strain, and $\phi(\theta)$ is an unknown function of θ. Then,

$$\sigma_{ij}(r,\theta) = Kr^{s-2}\tilde{\sigma}_{ij}(\theta) \tag{6a}$$

$$\varepsilon_{ij}(r,\theta) = \alpha K^n r^{n(s-2)}\tilde{\varepsilon}_{ij}(\theta) \tag{6b}$$

$$u_i(r,\theta) = \alpha K^n r^{n(s-2)+1}\tilde{u}_i(\theta) \tag{6c}$$

where the nondimensional $\tilde{\sigma}_{ij}(\theta)$, $\tilde{\varepsilon}_{ij}(\theta)$, and $\tilde{u}_i(\theta)$ are specific functions of $\tilde{\phi}$, $\tilde{\phi}'$, $\tilde{\phi}''$, n, and s. Hence these θ-variations of stresses, strains and displacements are known if s, $\tilde{\phi}$, and its derivatives are known for a prescribed n.

Substitution of (5) into the governing fourth order partial differential equation transforms it into a fourth order ordinary differential eigenvalue equation. For plane strain the eigen-equation is [4]

$$\left[(d^2/d\theta^2) - n(s-2)\{n(s-2)+2\}\right]\left[\tilde{\sigma}_e^{n-1}\{s(2-s)\tilde{\phi} + \tilde{\phi}''\}\right]$$
$$+ 4(s-1)\{n(s-2)+1\}(\tilde{\sigma}_e^{n-1}\tilde{\phi}')' = 0 \tag{7}$$

where $$\tilde{\sigma}_e \equiv \left[\frac{3}{4}\{\tilde{\phi}''^2 + 2(2-s)s\,\tilde{\phi}\tilde{\phi}'' + (2-s)^2 s^2\tilde{\phi}^2\} + 3(1-s)^2\tilde{\phi}'^2\right]^{1/2} \tag{8}$$

and $$()' \equiv (d/d\theta)$$

Equation (7) needs further manipulation into a form more amenable to solution. This form is highly non-linear and too complicated to present here. In symbolic form it is

$$\tilde{\phi}'''' = \tilde{\phi}''''(\tilde{\phi}, \tilde{\phi}', \tilde{\phi}'', \tilde{\phi}''', s, n, \theta) \tag{9}$$

Equation (9), subject to boundary conditions in Figure 1, can be solved in grains I and II by the shooting method. First (9) is transformed into a set of four first order ordinary differential equations which are solved simultaneously in both grains as initial value problems. The method consists of starting with a complete set of initial conditions of both known and guessed quantities on the horizontal boundaries, and integrating toward the slanted boundary. There the computed values from the two grains will usually not agree with the prescribed conditions. The mismatches are then considered as functions of the guessed initial conditions on the horizontal boundaries and are systematically eliminated by repeatedly readjusting the guessed boundary conditions and reintegrating, leading finally to the correct solution throughout. The numerical integration was performed by a fourth order Runge-Kutta method, and a Newton-Raphson scheme was used as a negative feedback to efficiently correct the guessed initial values.

Solutions of the dominant stress singularity showing the variation of s with n (dotted curve) and the variation of $\tilde{\sigma}_{ij}(\theta)$ with θ for two values of n are given in Figures 2, 5 and 6. Since the governing equation is homogeneous in $\tilde{\phi}$ and its derivatives, the variation with θ of the stresses plotted in Figures 5 and 6 are determinable only to within a constant multiplier which in these figures is chosen to give $\tilde{\phi}(0)=1$. On the other hand s which sets the singularity is completely determined.

For n=1, this problem is also solved in closed form by utilizing the method of Williams [5]. This analytical solution for n=1 serves as a useful check on the accuracy of the numerical shooting method. For n=1 both solutions agree to at least within 5 significant figures. The curves s=2 and s=(2n-1)/n in Figure 2 bound the region of acceptable eigenvalues. For s>2 there is no singularity and for s<(2n-1)/n the displacements are unbounded at the origin.

Stresses at Inclusions Corners

Figure 3 shows a lenticular rigid inclusion with an apex half angle ω (wetting half angle) along a sliding horizontal grain boundary subjected to uniform shear at infinity. As before, it is assumed that all boundaries, grain or interface, support no shear traction. The solution technique for the singular field at the apex is similar to that of the triple point with the added simplicity that one region now is rigid. The

results for the eigenvalues s (dotted curve) and the $\tilde{\sigma}_{ij}(\theta)$ are presented in Figures 4, 7 and 8 , for a wetting half angle $\omega=\pi/3$. Solutions in Figures 7 and 8 have been normalized such that $\tilde{\phi}(\theta_o=\pi-\omega)=1$. Once again, the solution for n=1 is also solved in closed form and compares equally well with the numerical results.

DISCUSSION

Figures 2 and 4 show that, for both the triple point and the inclusion, as n increases and the material becomes less strain rate sensitive the stress singularity relaxes and the strain singularity increases. In the limit as $n\to\infty$ and $s\to 2$ the material becomes rigid plastic, the stress singularity disappears (σ_{ij} independent of r) and the strain becomes nonunique ($\varepsilon_{ij}\to r^{\infty\cdot 0}$).

For the triple point problem, Figures 5 and 6 show that: $\tilde{\sigma}_e$ is comparatively small and constant in grain II making it act as if it were rigid, and that $\tilde{\sigma}_{r\theta}$ is maximum at the extension of the slanted boundaries which coincides with the incidence of folds in such locations [6]. Furthermore $\tilde{\sigma}_{\theta\theta}$ is maximum at $\theta=0$ where cracks are expected to appear. For the inclusion problem, Figures 7 and 8 show that $\tilde{\sigma}_{\theta\theta}$ is maximum at the slanted inclusion interface with the matrix, again coinciding with the position where microcracks are expected to form.

The amplitude K of the singularity field for both problems depends on the particular far field boundary condition and can be obtained by a global analysis utilizing, for example, the finite element method. Since for small grain specimens and large n the range of the singularity is of the order of the grain size, a good estimate of K can be obtained by equating the integral of the singular stress distribution over a characteristic repeat distance to that of the uniform distant traction. It is easy to show that for the triple point problem under a far field tensile stress σ_∞, K obtained in this manner is

$$K = \frac{3}{2}(s-1)\,\frac{\sigma_\infty}{\tilde{\sigma}_{\theta\theta}(0)}\left[\frac{d}{2\sqrt{3}}\right]^{2-s} \qquad (10)$$

where d is the grain size, $\tilde{\sigma}_{\theta\theta}(0)$ the value of $\tilde{\sigma}_{\theta\theta}$ at $\theta=0$ shown in Figures 3 and 4, and s is given in Figure 2 for the appropriate n.

The results presented here are part of a very general study of crack initiation at interfaces in creep which will be published elsewhere.

ACKNOWLEDGEMENT

This research has been supported by the Army Research Office under contract No. DAAG29-74-C-0008.

REFERENCES

1. GRANT, N. J., Fracture Vol. III, ed. H. Liebowitz, Academic Press, N.Y., 1971, 483.
2. PERRY, A. J., J. Mat. Sci., 9, 1974, 1016.
3. TAKEUCHI, S. and ARGON, A. S., J. Mat. Sci., 11, 1976, 1542.

4. HUTCHINSON, J. W., J. Mech. Phys. Solids, 16, 1968, 13.
5. WILLIAMS, M. L., J. Appl. Mech., Trans. ASME, 74, 1952, 526.
6. GRANT, N. J. and CHAUDHURI, A. R., Deformation and Fracture at Elevated Temperatures, ed. N. J. Grant and A. W. Mullendore, M.I.T. Press, Cambridge, 1965, 105.

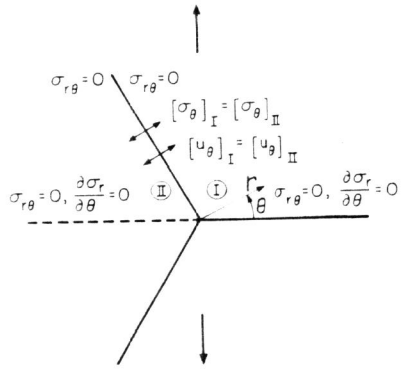

Figure 1 Boundary Conditions at Triple Point Junction Subject to Far Field Tensile Loading

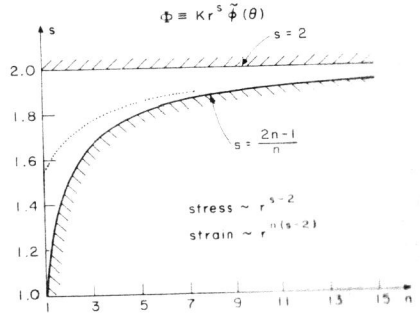

Figure 2 The Variation of s with n, Triple Point Problem

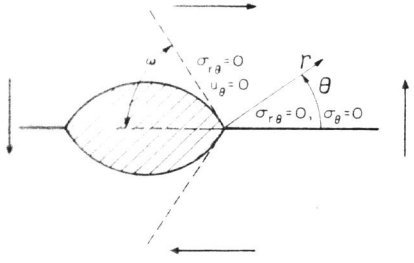

Figure 3 Boundary Conditions at Apex of Rigid Inclusion Situated in a Free Sliding Grain Boundary Subject to Far Field Shearing

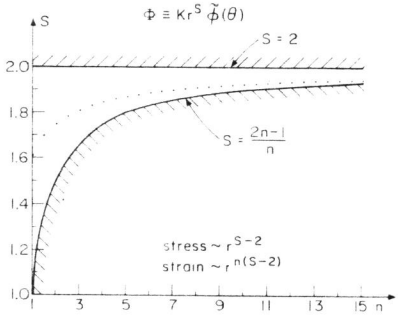

Figure 4 The Variation of s with n, Inclusion Problem with $\omega = 60°$

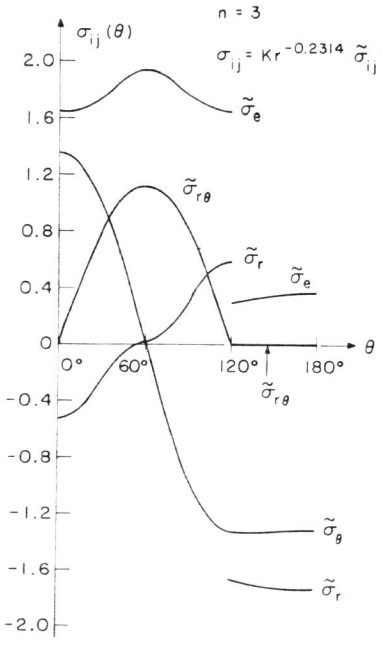

Figure 5 Plain Strain $\tilde{\sigma}_{ij}(\theta)$ versus θ at Triple Point, n = 3

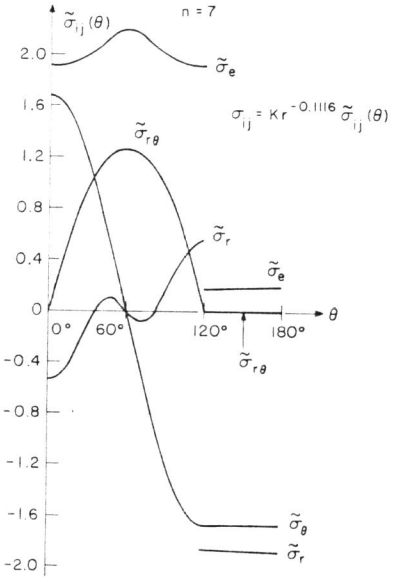

Figure 6 Plain Strain $\tilde{\sigma}_{ij}(\theta)$ versus θ at Triple Point, n = 7

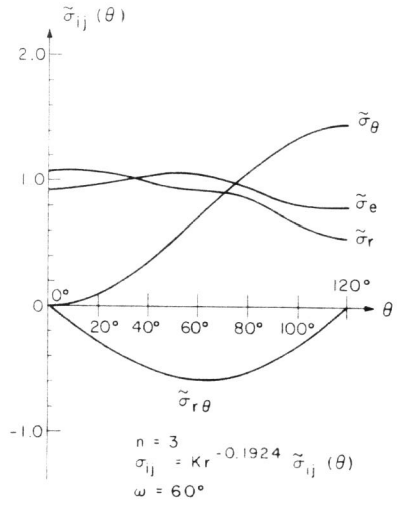

Figure 7 Plain Strain $\tilde{\sigma}_{ij}(\theta)$ versus θ at Apex of Inclusion, n = 3

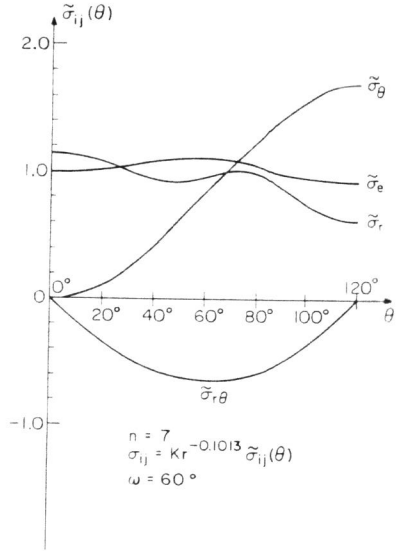

Figure 8 Plain Strain $\tilde{\sigma}_{ij}(\theta)$ versus θ at Apex of Inclusion, n = 7